

Probing Proton Strangeness with Time-Like Virtual Compton Scattering

Stephen R. Cotanch

Department of Physics, North Carolina State University, Raleigh, NC 27695 USA

Robert A. Williams

*Nuclear Physics Group, Hampton University, Hampton, VA 23668 USA
and*

Jefferson Lab, 12000 Jefferson Avenue, Newport News, VA 23606 USA

PACS: 12.40Nn, 12.40Vv, 13.40.Gp, 13.40.Hq, 13.60Fz, 13.60.Le, 13.60.-r

Keywords: Compton scattering, ϕ photoproduction, vector meson dominance, nucleon form factors, nucleon strangeness, ϕN coupling.

Abstract

We document that $p(\gamma, e^+e^-)p$ measurements will yield new, important information about the off-shell time-like nucleon form factors, especially in the ϕ meson region ($q^2 = M_\phi^2$) governing the ϕN couplings $g_{\phi NN}^{V,T}$. Calculations for $p(\gamma, e^+e^-)p$, utilizing vector meson dominance, predict measurable ϕ enhancements at high $|t|$ compared to the expected ϕ background production from π , η and Pomeron exchange. The ϕ form factor contribution generates a novel experimental signature for OZI violation and the proton strangeness content. The ϕN couplings are determined independently from a combined analysis of the neutron electric form factor and recent high $|t|$ ϕ photoproduction. The π , η and Pomeron transition form factors are also predicted and the observed π and η transition moments are reproduced.

Compton scattering, an elegant time-honored topic, is an effective probe of hadron structure. In this paper we calculate a striking effect for a less investigated version of this process, time-like virtual Compton scattering [TVCS], $p(\gamma, e^+e^-)p$. Invoking vector meson dominance [VMD], we predict distinctive, dual peaked cross section resonances for time-like virtual photon four-momentum spanning the vector meson masses ($q^2 \sim M_V^2$ for $V = \rho, \omega, \phi$). In our Quantum Hadrodynmaic [QHD] model these narrow, order of magnitude enhancements arise from vector mesons, associated with the outgoing virtual photon, coupling in the t channel to π, η and Pomeron \mathcal{P} exchanges, and also to the proton through the time-like form factors (F_1^p, F_2^p or G_E^p, G_M^p) in the s and u channels. There is no nucleon form factor data for $0 \leq q^2 \leq 4M_p^2$ since all measurements to date have utilized the two-body annihilation processes $e^+e^- \leftrightarrow N\bar{N}$. However, $p(\gamma, e^+e^-)p$ involves a three-body final state with an essentially unrestricted virtual photon mass $q^2 \geq 4M_e^2 \sim 0$. The dramatic VMD resonant signature was also noted in our previous analyses [1,2] of $p(\pi^-, e^+e^-)n$ for experiments with hadron beams. This work extends that study and affirms TVCS measurements at electromagnetic facilities can provide similar information.

Knowledge of the nucleon time-like form-factors, for both on and off-shell nucleons, permits a direct assessment of the nucleon strangeness content. Nucleon strangeness is quantified by the nucleon matrix elements, $\langle N|\bar{s}\Gamma_n s|N\rangle$, involving the $n = 1, 2, \dots, 16$ Lorentz bilinear covariants. Here we address the vector and tensor elements, γ_μ and $\sigma_{\mu\nu}$, which respectively corresponds to the coupling constants $g_{\phi NN}^V$ and $g_{\phi NN}^T$, since the ϕ is predominantly $s\bar{s}$. These coupling constants completely specify the QHD ϕNN Lagrangian

$$\mathcal{L}_{\phi NN} = g_{\phi NN}^V \bar{N} \gamma_\mu N \phi^\mu + g_{\phi NN}^T \bar{N} \sigma_{\mu\nu} N [\nabla^\mu \phi^\nu - \nabla^\nu \phi^\mu] \quad (1)$$

which we use for our cross section predictions presented below. By extracting these couplings from the nucleon form factors using VMD and from non-diffractive ϕ photoproduction [3–5], one can quantify the hidden strangeness in the nucleon. Clearly if the probability of an $s\bar{s}$ pair in the proton is zero or extremely small, ϕN coupling will be significantly suppressed due to the dominant $s\bar{s}$ structure of the ϕ and the OZI rule [6] (i.e. suppressed interactions between hadrons with different quark flavors). However, sizeable OZI violations (ϕ production/coupling assuming $\langle N|\bar{s}\Gamma_n s|N\rangle = 0$) have been observed in $p\bar{p}$ annihilation experiments at LEAR by the ASTERIX, Crystal Barrel and OBELIX collaborations [7]. These results are consistent with analyses of other independent experiments such as the EMC deep inelastic μp scattering [8], elastic νp scattering at BNL [9] and measurements of the πN sigma term [10] which all support an appreciable strangeness component in the proton. Reference [11] reviews the evidence for hidden strangeness.

Theoretically, there have been several strangeness calculations [5,12–17] of both ϕN couplings and nucleon properties (spin, radius, magnetic moment) using a variety of approaches. Many of these analyses have been formulated in terms of hyperon Fock components for the nucleon, $|KY\rangle (Y = \Lambda, \Sigma)$, and/or meson loop contributions using dispersion relations. While loop cancellations are appreciable, theoretical uncertainty precludes a robust quantitative assessment of strangeness and additional study appears necessary. We will also address this in a future communication using a many-body, relativistic field theoretical quark/gluon formalism that implements chiral symmetry [18].

Here we adopt a phenomenological approach which directly determines the ϕN couplings from data and then predicts $p(\gamma, \gamma_v)p$. We first compute the hadron form factors utilizing a generalization [19,20] of the VMD model developed in ref. [21]. The $SU_F(3)$ symmetry relations and Sakurai’s universality hypothesis are incorporated to describe the baryon octet EM form factors. A good description of the data is obtained using the specific vector meson-nucleon couplings, $C_\rho(N) = 0.4$, $C_\omega(N) = 0.2$ and $C_\phi(N) = -0.1$, where $C_V(N) = g_{VNN}/f_V$ is the ratio of the vector meson-nucleon hadronic coupling, g_{VNN} , to the meson-leptonic decay constant, f_V . From the $\phi \rightarrow e^+e^-$ decay width we extract the ϕ decay constant, $f_\phi = -13.1$, yielding the ϕN vector coupling, $g_{\phi NN}^V = 1.3$. Because of its relatively small size, the neutron electric form factor, G_E^n , is very sensitive to ϕN coupling. As Fig. 1 indicates, there is considerable uncertainty to both the vector and tensor, $g_{\phi NN}^T = \frac{\kappa_\phi^T}{M_\phi} g_{\phi NN}^V$, coupling constants. New, but still preliminary, G_E^n data indicates an even smaller form factor which suggests a larger ϕN coupling (inverse relation). Clearly, a precision G_E^n measurement will significantly constrain the values of $g_{\phi NN}^V$ and tensor moment κ_ϕ^T . However, by analyzing recent ϕ photoproduction data (see below) we have reduced part of this uncertainty leading to the values $g_{\phi NN}^V = 1.3$, $g_{\phi NN}^T = 2.3$ and $\kappa_\phi^T = 1.8$. Our vector ϕN coupling constant relative to ωN is $g_{\phi NN}^2/g_{\omega NN}^2 = 0.14$, slightly smaller but still consistent with ref. [3].

We also use VMD for the meson transition form factors entering the t channel cross section contributions. While the proton’s strangeness content remains uncertain, the u and d quark components of the ϕ and η are much better known (see below). The pseudoscalar, $\gamma\pi \rightarrow \gamma_v$, $\gamma\eta \rightarrow \gamma_v$ and Pomeron, $\gamma\mathcal{P} \rightarrow \gamma_v$ transition form factors are computed from ρ , ω and ϕ vector meson propagators with couplings determined directly from the $\phi \rightarrow \gamma\pi$, $\phi \rightarrow \gamma\eta$, $\omega \rightarrow \gamma\pi$, $\omega \rightarrow \gamma\eta$, $\rho \rightarrow \gamma\pi$ and $\rho \rightarrow \gamma\eta$ decay widths [22]. The leptonic decays $\phi \rightarrow e^+e^-$ and $\omega \rightarrow e^+e^-$ together with the photon radiative decays $\pi \rightarrow \gamma\gamma$ and $\eta \rightarrow \gamma\gamma$ provide a consistency check on the VMD π and η transition form factors because of the normalization conditions

$$\kappa_{\pi\gamma\gamma} = \frac{\kappa_{\rho\pi\gamma}}{f_\rho} + \frac{\kappa_{\omega\pi\gamma}}{f_\omega} + \frac{\kappa_{\phi\pi\gamma}}{f_\phi}, \quad \kappa_{\eta\gamma\gamma} = \frac{\kappa_{\rho\eta\gamma}}{f_\rho} + \frac{\kappa_{\omega\eta\gamma}}{f_\omega} + \frac{\kappa_{\phi\eta\gamma}}{f_\phi}. \quad (2)$$

Using the most recent data [22] VMD predicts the moments $\kappa_{\pi\gamma\gamma} = 0.30$, $\kappa_{\eta\gamma\gamma} = 0.27$, $\kappa_{\rho\gamma\gamma} = 0.11$ which are in excellent agreement with the observed values $\kappa_{\pi\gamma\gamma} = 0.27$, $\kappa_{\eta\gamma\gamma} = 0.26$ ($\kappa_{\rho\gamma\gamma}$ has not been measured). The VMD couplings are summarized in Table I. The Pomeron radiative transition moments have been extracted from a ϕ photoproduction analysis [23].

Table I. Vector meson transition moments and decay constants.

V	$\kappa_{V\pi\gamma}$	$\kappa_{V\eta\gamma}$	$\kappa_{V\rho\gamma}$	f_V
ρ	0.901	1.470	0.62	5.0
ω	2.324	0.532	0.62	17.1
ϕ	0.138	0.715	0.62	-13.1

Figures 2 and 3 display our calculated proton form factors along with available data. Note for $q^2 = 1.0 \text{ GeV}^2 \cong M_\phi^2$, both G_E^p and G_M^p exhibit significant, narrow resonances. In the OZI limit (zero ϕ coupling), the form factors are essentially unchanged in the space-like region and the time-like ϕ peaks vanish. The absolute values are plotted since the form factors are complex in the vector meson region. The neutron time-like form factor behavior is similar but, as discussed above, space-like G_E^n is very sensitive to $C_\phi(N)$.

Since ϕ photoproduction and TVCS have the same quantum numbers, $\gamma(q, \lambda) + p(p, \sigma) \rightarrow V(q', \lambda') + p(p', \sigma')$, $V = \phi$ or γ_v , the cm cross section for both is

$$\frac{d\sigma}{dt} = \frac{M_p^2 (\hbar c)^2}{64\pi s |\mathbf{q}|^2} \sum_{\lambda' \lambda \sigma' \sigma} |T_{\lambda' \sigma' \lambda \sigma}|^2, \quad (3)$$

with q , p , and λ , σ , denote the corresponding 4-momenta and helicities, respectively. The photoproduction helicity amplitude, $T_{\lambda' \sigma' \lambda \sigma}$, is

$$T_{\lambda' \sigma' \lambda \sigma} \equiv \epsilon_\mu(\lambda) \phi_\nu^*(\lambda') \mathcal{H}_{\sigma' \sigma}^{\mu \nu}, \quad (4)$$

where $\epsilon_\mu(\lambda)$ and $\phi_\nu^*(\lambda')$ are the initial photon and final virtual photon (or ϕ) polarization 4-vectors in the helicity basis, respectively. The hadronic current tensor, $\mathcal{H}_{\sigma' \sigma}^{\mu \nu}$, is evaluated at tree level from the s , t and u channel QHD diagrams. Working in the cm system ($\mathbf{q} + \mathbf{p} = \mathbf{q}' + \mathbf{p}' = \mathbf{0}$), with the z-axis along \mathbf{q} , the photon polarization vectors are

$$\epsilon_\mu(\lambda) = -\frac{\lambda}{\sqrt{2}}(0, 1, i\lambda, 0) \quad (\lambda = \pm), \quad (5)$$

$$\phi_\mu^*(\lambda') = \frac{\lambda'}{\sqrt{2}}(0, -\cos \theta_{cm}, i\lambda', \sin \theta_{cm}) \quad (\lambda' = \pm), \quad (6)$$

$$\phi_\mu^*(\lambda') = \frac{1}{\sqrt{q'^2}}(|\mathbf{q}'|, q'_0 \sin \theta_{cm}, 0, q'_0 \cos \theta_{cm}) \quad (\lambda' = 0) . \quad (7)$$

Evaluating the QHD Lagrangian diagrams generates the following s, t and u channel contributions to the hadronic current tensor.

t channel 0^+ Pomeron (\mathcal{P}) exchange:

$$\mathcal{H}_{\sigma'\sigma}^{\mu\nu} = \Gamma_{\mathcal{P}} \Pi_{\mathcal{P}}(t) \left(\frac{s - s_{th}}{s_0} \right)^{\alpha(t)} \bar{u}(p', \sigma') u(p, \sigma) [q \cdot q' g_{\mu\nu} - q'_\mu q'_\nu] . \quad (8)$$

t channel 0^- meson ($x = \pi^0, \eta$) exchange:

$$\mathcal{H}_{\sigma'\sigma}^{\mu\nu} = \frac{\Gamma_x F_t(t; \lambda)}{M_\phi [(p' - p)^2 - M_x^2]} \bar{u}(p', \sigma') \gamma_5 u(p, \sigma) \epsilon^{\mu\alpha\nu\beta} q_\alpha q'_\beta . \quad (9)$$

s channel proton (p) propagation:

$$\begin{aligned} \mathcal{H}_{\sigma'\sigma}^{\mu\nu} = & \bar{u}(p', \sigma') [\Gamma'_1 \gamma^\nu + i\Gamma'_2 \sigma^{\nu\alpha} q'_\alpha] \\ & \times \frac{(p + q) \cdot \gamma + M_p}{(p + q)^2 - M_p^2 + \Sigma_p(s)} [\Gamma_1 \gamma^\mu + i\Gamma_2 \sigma^{\mu\beta} q_\beta] u(p, \sigma) . \end{aligned} \quad (10)$$

u channel channel proton (p) propagation:

$$\begin{aligned} \mathcal{H}_{\sigma'\sigma}^{\mu\nu} = & \bar{u}(p', \sigma') [\Gamma_1 \gamma^\mu + i\Gamma_2 \sigma^{\mu\beta} q_\beta] \\ & \times \frac{(p' - q) \cdot \gamma + M_p}{(p' - q)^2 - M_p^2 + \Sigma_p(u)} [\Gamma'_1 \gamma^\nu + i\Gamma'_2 \sigma^{\nu\alpha} q'_\alpha] u(p, \sigma) . \end{aligned} \quad (11)$$

The scalar (0^+) Pomeron coupling to the $\mathcal{P}NN$, $\bar{u}(p', \sigma')u(p, \sigma)$, and $\phi\mathcal{P}\gamma$, $F_{\mu\nu}^\gamma F_\phi^{\mu\nu}$, vertices is represented by $\Gamma_{\mathcal{P}}$, which is a product of Pomeron hadronic and electromagnetic coupling constants. The energy dependence, $(s/s_0)^{\alpha(t)}$, follows from Regge theory [24] with Pomeron trajectory, $\alpha(t) = .999 + .27 \text{ GeV}^{-2} t$, which reproduces established high energy diffractive data. To describe the less well known low energy dependence, we introduce the parameter s_{th} ($0 \leq s_{th} \leq s_0$). Taking the reference energy $\sqrt{s_0}$ as the production threshold, $s_0 = (M_V + M_p)^2$ ($M_V = \sqrt{q'^2}$ or M_ϕ for $V = \gamma_v$ or ϕ), we find the ϕ photoproduction data clearly selects the maximum value, $s_{th} \rightarrow s_0$. The Γ factors in Eqs. (8-11) are products of hadronic and electromagnetic coupling constants appropriate for either $V = \phi, \gamma_v$ and are listed in Table II.

Table II. Effective vertex couplings. $\Gamma_1 = e = \sqrt{(4\pi\alpha_e)}$, $\Gamma_2 = \frac{e\kappa_p}{2M_p}$, $\kappa_p = 1.793$, $g_{\mathcal{P}NN} = 44.0$, $g_{\pi NN} = 13.8$ and $g_{\eta NN} = 7.5$.

V	$\Gamma_{\mathcal{P}}$	Γ_{π}	Γ_{η}	Γ'_1	Γ'_2
ϕ	$g_{\mathcal{P}NN}(\frac{e\kappa_{\phi}\mathcal{P}\gamma}{M_{\phi}})$	$g_{\pi NN}(\frac{e\kappa_{\phi}\pi\gamma}{M_{\phi}})$	$g_{\eta NN}(\frac{e\kappa_{\phi}\eta\gamma}{M_{\phi}})$	$g_{\phi NN}$	$g_{\phi NN}(\frac{\kappa_{\phi}^T}{M_{\phi}})$
γ_v	$g_{\mathcal{P}NN}(\frac{e^2\kappa_{\mathcal{P}\gamma\gamma}}{M_{\phi}})$	$g_{\pi NN}(\frac{e^2\kappa_{\pi\gamma\gamma}}{M_{\phi}})$	$g_{\eta NN}(\frac{e^2\kappa_{\eta\gamma\gamma}}{M_{\phi}})$	$e F_1^p(q'^2)$	$(\frac{e\kappa_p}{2M_p})F_2^p(q'^2)$

The effective Pomeron propagator, $\Pi_{\mathcal{P}}(t)$, describes [23] scalar exchange

$$\Pi_{\mathcal{P}}(t) = \frac{e^{\beta t}}{t - M_{\mathcal{P}}^2}, \quad (12)$$

and reproduces the known diffractive t dependence using the lightest scalar glueball mass, $M_{\mathcal{P}} = 1.7 \text{ GeV}$, and Pomeron slope $\beta = .27 \text{ GeV}^{-2}$. The pseudoscalar t channel form factor, $F_t(t; \lambda)$, governs hadronic structure and is necessary for the correct 4-momentum transfer dependence in meson photoproduction [25,26]. Covariance and crossing symmetry are preserved using

$$F_t(t; \lambda) = \frac{\lambda^4 + t_{min}^2}{\lambda^4 + t^2}, \quad (13)$$

normalized to unity at $t_{min} = t$ ($\theta_{\gamma\phi}^{c.m.} = 0$). From $p(\gamma, \phi)p$ data, the optimum cutoff parameter is $\lambda = 0.7 \text{ GeV}$. For the s and u channels we describe the off-shell proton by a self-energy correction, Σ_p , to the propagator. To maintain both gauge invariance and the correct on-shell proton mass, Σ_p must vanish at the proton pole and also be an odd function of $(s - M_p^2)$

$$\Sigma_p(s) = \alpha_{off} \frac{(s - M_p^2)^3}{M_p^4}. \quad (14)$$

The dimensionless off-shell parameter, $\alpha_{off} = 1.29$, was also adjusted for optimal agreement with recent, and higher $|t|$, ϕ photoproduction data [27] shown in Fig. 4. Note the sensitivity and relative contributions from the $|t|$ channel Pomeron \mathcal{P} (dense dotted curve), π (short dashed curve), η (spare dotted curve) and s channel ϕN coupling (long dashed curve). Since the t channel processes are suppressed at high $|t|$, the latest data permits more stringent constraints on the ϕN coupling, yielding the values quoted above. It would be extremely useful to have measurements for $|t| > 4 \text{ GeV}^2$ where our model predicts an enhancement from interference between the vector and tensor ϕN couplings.

Figures 5 and 6 represent our key results and display the TVCS cross sections versus final proton lab angle and initial photon lab energy, respectively. Notice in Fig. 5 the dual peak resonant signature due to the quadratic relation between q^2 and recoil proton lab angle. The smaller angle ϕ peak, corresponding to high $|t|$, is dominated by the u channel (proton propagator) $g_{\phi NN}$ coupling (dense dotted curve labeled p). This is our prediction for measuring the proton strangeness content. The two other peaks near 25° and 30° , have lower $|t|$ and respectively represent ϕ and ω coupling to mesons in t channel exchange. These two peaks embody established results and therefore constitute the expected ϕ production background. Figure 6 demonstrates the cross section energy dependence at maximum $|t|$ on the ϕ resonance ($q^2 = M_\phi^2$). Our model clearly predicts u channel domination (curve labeled p) above 2.5 GeV lab energy, enabling direct extraction of $g_{\phi NN}$.

We wish to stress that our ϕ dual peak signature and magnitude follows from VMD only and is independent of the underlying dynamical model. While our results utilized QHD, we submit similar findings will occur for other models. Assuming only the validity of VMD, we confidently predict that a measurement of the high $|t|$ TVCS cross section ratio $R = \sigma(q^2 = M_\phi^2)/\sigma(q^2 = M_\omega^2)$ would yield a result proportional to $g_{\phi NN}^2/g_{\omega NN}^2$. We have confirmed this numerically in our model, $R = 0.14 f$ (where f is a kinematic quantity of order unity). This is over an order of magnitude larger than the OZI (no nucleon strangeness) prediction [11], $R = \tan^2 \delta f = 0.0042 f$, where $\delta = 3.7^\circ$ is the deviation from the ideal quark flavor mixing angle in the ϕ . Thus, TVCS experiments are an excellent means for probing the proton strangeness content.

Note also that TVCS probes the (half) off-shell proton form factors which, depending on kinematics, can be quite different from the on-shell form factors used in this study. Reference [28] addresses this issue further, including ambiguity in off-shell formulation. Here we simply point out that both on and off-shell form factors contain important information about ϕN coupling in the time-like region and that the above ratio R will be less sensitive than the form factors to off-shell effects. Also, by comparing the TVCS off-shell form factors to the known on-shell G_E^p , G_M^p for $q^2 \geq 4M_p^2$, off-shell effects can be directly assessed. A complete analysis also requires N^* resonances. However, by choosing large s and $|t|$ kinematics with $u \approx 0$, only the lightest baryon resonances will compete with the proton Born term $1/(u - M_p^2)$. Related, ref. [28] also details how the Bethe-Heitler process can be exploited to extract the TVCS amplitude by measuring the e^+e^- asymmetry.

Lastly, we have performed TVCS calculations for $n(\gamma, \gamma_v)n$ and find similar results, now involving the neutron form factors. Hence by measuring $d(\gamma, \gamma_v)d$, complimentary neutron strangeness information can also be obtained.

Summarizing, we have shown that VMD provides a good comprehensive description of meson and nucleon electromagnetic observables and that both ϕ photoproduction and TVCS are sensitive to VMD parameters. In particular, TVCS allows probing the better known π , η and \mathcal{P} t channel exchanges at low $|t|$ as well as the uncertain u channel ϕN coupling at high $|t|$. Further, the TVCS process is ideal for investigating the time-like nucleon form factor which is currently not known below $q^2 = 4M_N^2 \sim 3.5 \text{ GeV}^2$. Assuming the validity of VMD with ϕN couplings, we predict narrow, dual peak e^+e^- (and also $\mu^+\mu^-$) resonances that should be clearly observable. These order of magnitude enhancements represent a novel experimental signature for both confirming the validity of VDM for the ρ and ω , which is anticipated, and also for quantifying the ϕN coupling governing the proton's hidden strangeness.

This work was partially supported by grants DOE DE-FG02-97ER41048 and NSF INT-9807009. Contributions from Zach Hill are also appreciated.

References

- [1] R. A. Williams and S. R. Cotanch, Phys. Rev. Lett. 77 (1996) 1008.
- [2] S. R. Cotanch and R. A. Williams, Nucl. Phys. A631 (1998) 478.
- [3] J. Ellis, E. Gabathuler, and M. Karliner, Phys. Lett. B217 (1989) 173.
- [4] E. M. Henley, G. Krein, S. J. Pollock, and A. G. Williams, Phys. Lett. B269 (1991) 31; E. M. Henley, G. Krein, and A. G. Williams, Phys. Lett. B281 (1992) 178.
- [5] A. I. Titov, S. N. Yang, and Y. Oh, Nucl. Phys. A618 (1997) 659; Phys. Rev. Lett. 79 (1997) 1634.
- [6] S. Okubo, Phys. Lett. B5 (1963) 165; G. Zweig, CERN Report 8419/TH412 (1964); I. Iizuka, Prog. Theor. Phys. 38 (1966) 21.
- [7] ASTERIX Collaboration, J. Reifenrother *et al.*, Phys. Lett. B267 (1991) 299; Crystal Barrel Collaboration, M. A. Faessler *et al.*, Phys. At. Nuclei 57 (1994) 1693; OBELIX Collaboration, V. G. Ableev *et al.*, Phys. At. Nuclei 57 (1994) 1716; Phys. Lett. B334 (1994) 237.
- [8] EMC Collaboration, J. Ashman *et al.*, Phys. Lett. B206 (1988) 364.
- [9] L. A. Ahrens *et al.*, Phys. Rev. D 35 (1987) 785.
- [10] J. F. Donoghue and C. R. Nappi, Phys. Lett. B168 (1986) 105; J. Gasser, H. Leutwyler, and M. E. Sainio, *ibid.* (1991) 252.
- [11] J. Ellis, M. Karliner, D. E. Kharzeev, and M. G. Sapozhnikov, Phys. Lett. B353 (1995) 319.

- [12] P. Geiger and N. Isgur, Phys. Rev. Lett. 67 (1991) 1066; Phys. Rev. D 55 (1997) 299.
- [13] D. B. Leinweber, Nucl. Phys. A585 (1995) 341c.
- [14] W. Melnitchouk and M. Malheiro, Phys. Rev. C 55 (1997) 431.
- [15] M. J. Savage and J. Walden, Phys. Rev. D 55 (1997) 5376.
- [16] M. J. Musolf and H.-W. Hammer, and D. Drechsel, Phys. Rev. D 55 (1997) 2741; Erratum-ibid. D 62 (2000) 079901.
- [17] Ulf-G. Meißner, V. Mull, J. Speth, and J. W. Van Orden, Phys. Lett. B408 (1997) 381.
- [18] F. J. Llanes-Estrada and S. R. Cotanch, Phys. Rev. Lett. 84, 1102 (2000); Nucl. Phys. A697 (2002) 303.
- [19] R. A. Williams, S. Krewald, and K. Linen, Phys. Rev. C 51 (1995) 566.
- [20] R. A. Williams and C. Pickett-Truman, Phys. Rev. C 53 (1996) 1580.
- [21] M. Gari and W. Krümpelmann, Phys. Lett. B274 (1992) 159.
- [22] Particle Data Group, Eur. Phys. J. C 15 (2000) 1-877.
- [23] R. A. Williams, Phys. Rev. C57 (1998) 223.
- [24] P. D. B. Collins, “*An introduction to Regge theory and high energy physics*”, Cambridge University Press, Cambridge, 1977.
- [25] Z. Li, Phys. Rev. C52 (1995) 1648.
- [26] D. Lu, R. H. Landau, and S. C. Phatak, Phys. Rev. C52 (1995) 1662.
- [27] CLASS Collaboration, E. Anciant *et al.*, Phys. Rev. Lett. 85 (2000) 4682.
- [28] A. Yu. Korchin, O. Scholten, and F. de Jong, Phys. Lett. B402 (1997) 1.

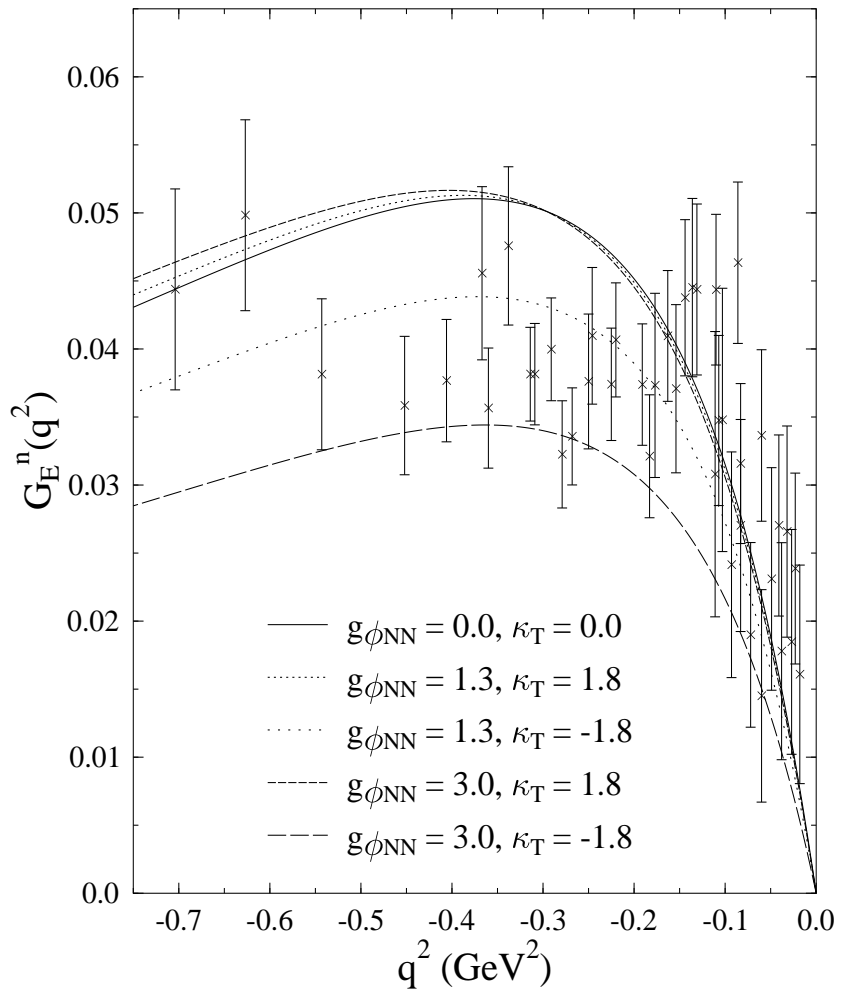


Fig. 1. Data and VMD for the neutron space-like electric form factor. The curves reflect sensitivity to ϕN coupling.

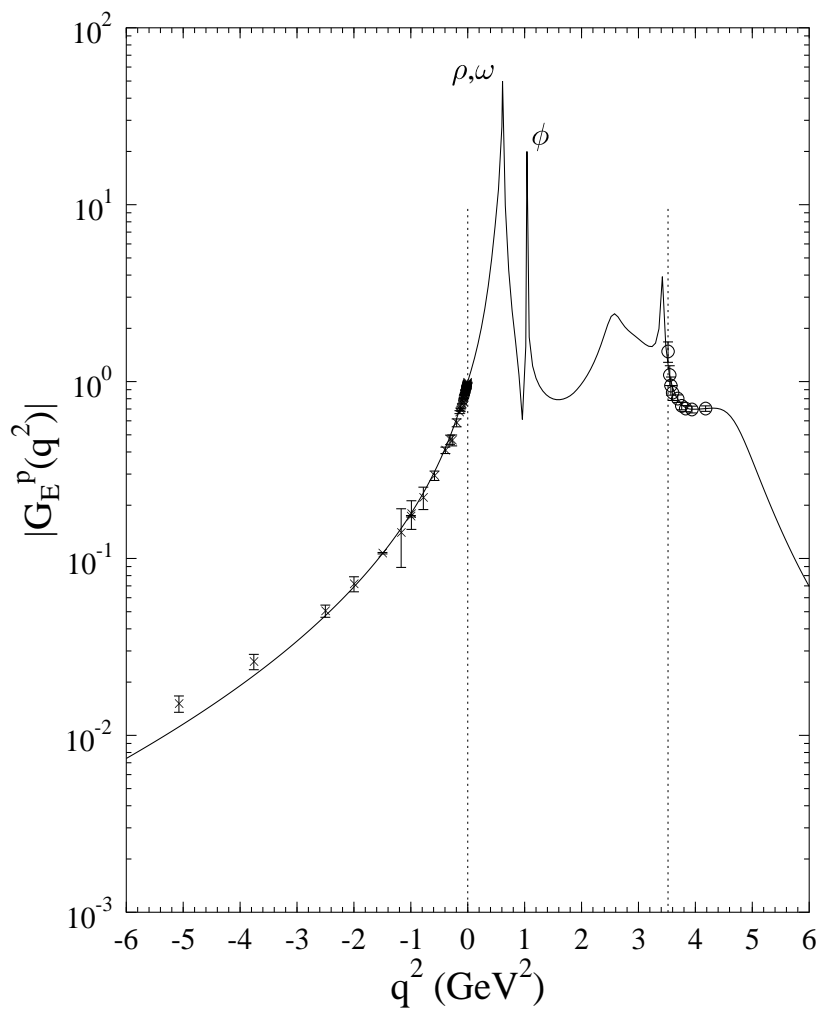


Fig. 2. Data and VMD (absolute value) for the proton electric form factor. Note the resonant peaks in the unmeasured time-like vector meson region.

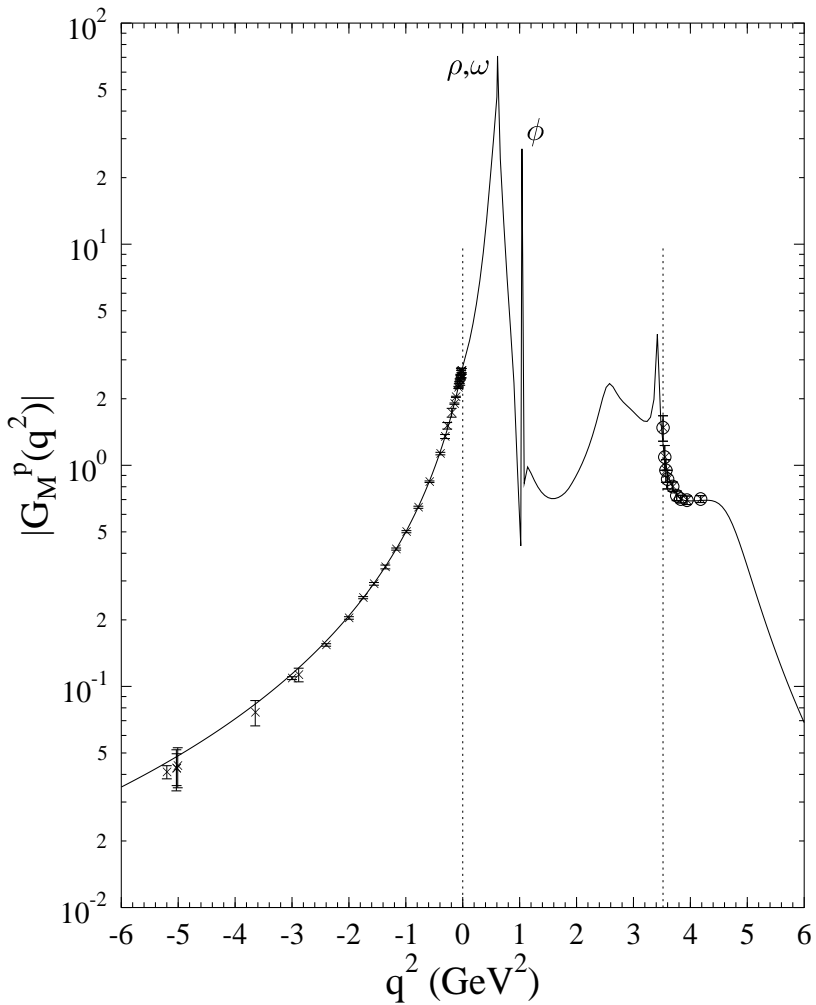


Fig. 3. Data and VMD (absolute value) for the proton magnetic form factor.

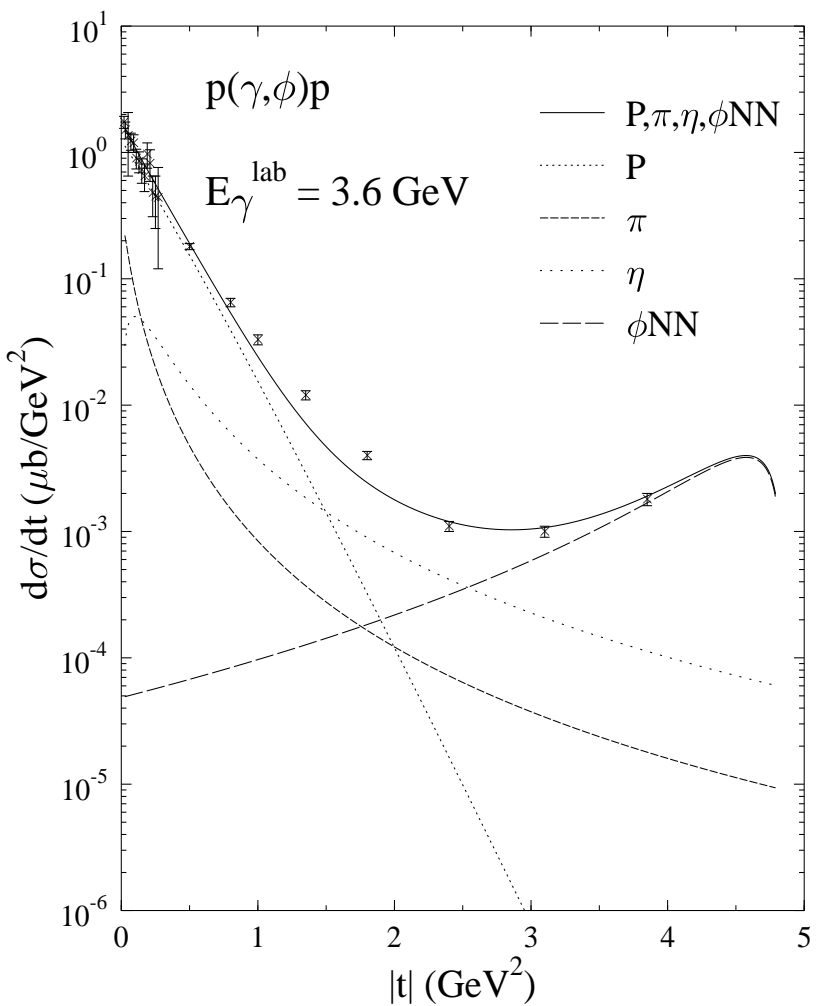


Fig. 4. Theory and data for ϕ photoproduction, $p(\gamma, \phi)p$.

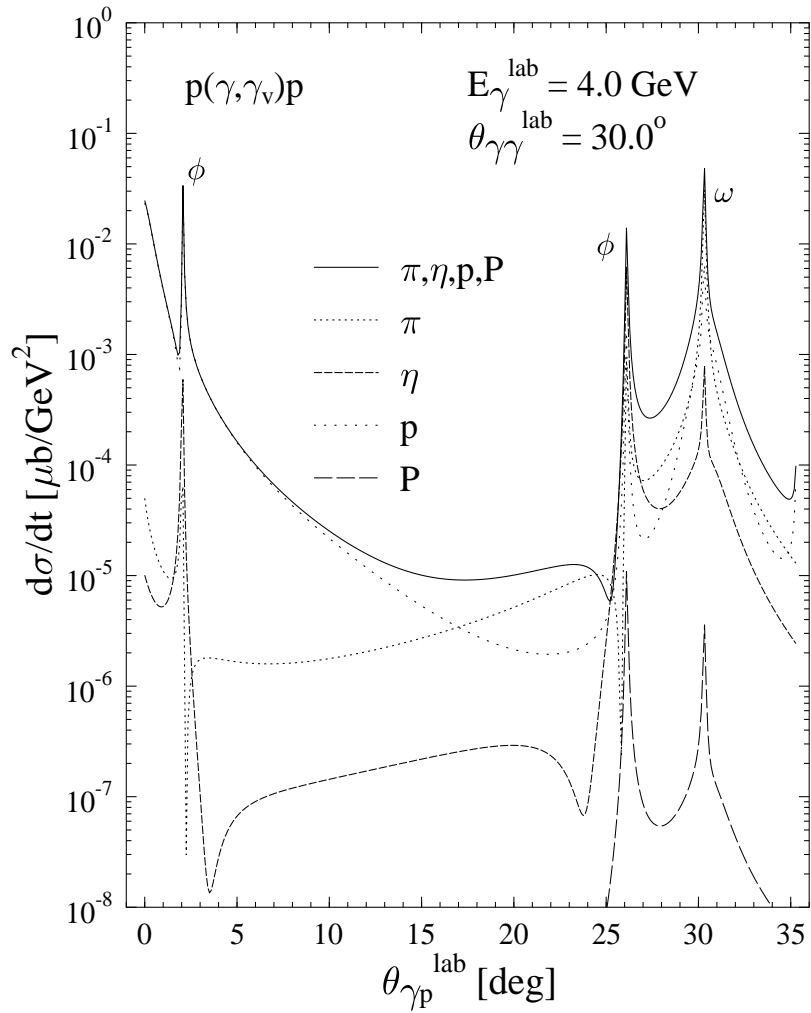


Fig. 5. VMD prediction for TVCS, $p(\gamma, \gamma_v)p$, showing dual peak resonances. The smaller angle ϕ peak is from ϕN coupling and quantifies the proton's strangeness.

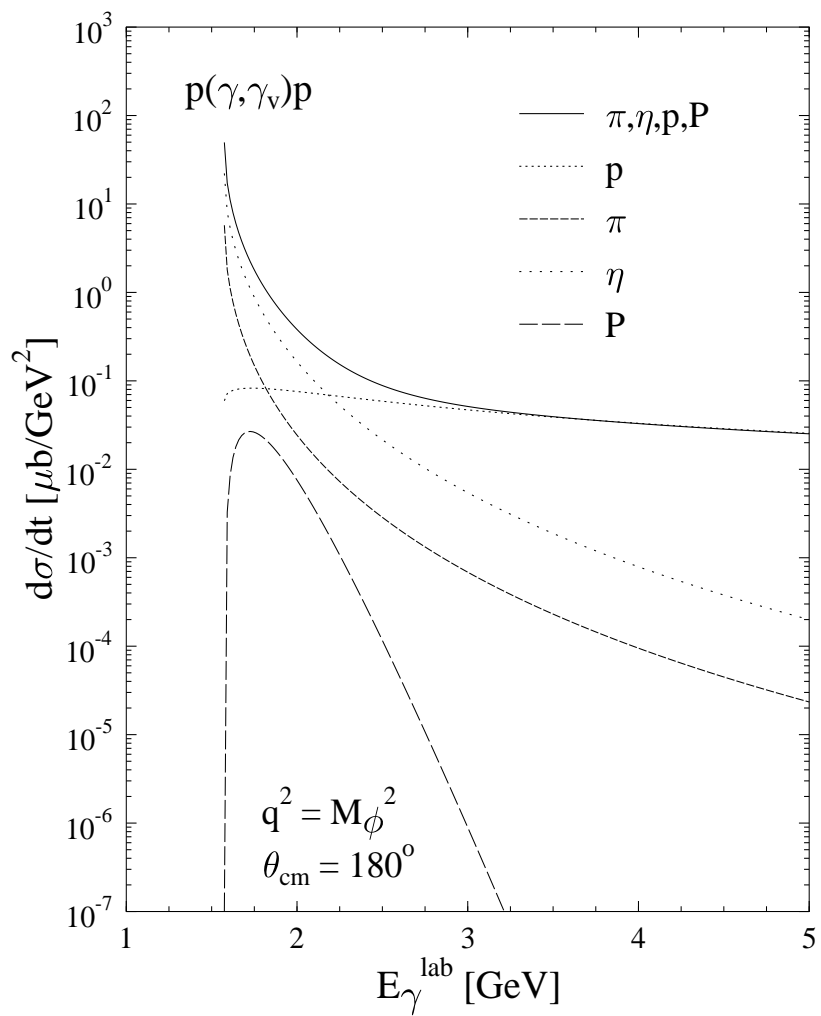


Fig. 6. VMD prediction for $p(\gamma, \gamma_v)p$ versus lab energy. The higher energy cross section is dominated by ϕN coupling (dense dotted line).